JOURNAL OF PROPULSION AND POWER
Vol. 18, No. 1, January–February 2002

Experimental Investigation of Limit-Cycle Oscillations in an Unstable Gas Turbine Combustor

Tim C. Lieuwen*
Georgia Institute of Technology, Atlanta, Georgia 30332-0150

This paper describes an experimental investigation of limit-cycle oscillations in an unstable gas turbine combustor simulator. This investigation was performed to improve the current understanding of the characteristics of these oscillations and the nonlinear processes that affect them. Such an understanding is needed in order to predict instability amplitudes, to aid in correlating data, and to develop and optimize active control methodologies. The paper first describes an analysis of the statistical and temporal features of the limit-cycle pressure oscillations and discusses the role of noise and system nonlinearities upon these oscillations. Next, it discusses the important role that the combustor inlet velocity plays in determining the amplitude of the limit-cycle oscillations. The paper also presents data illustrating the characteristics of the combustor's transition from stable to unstable operation. Finally, it is shown that inherent noise in the system can strongly affect the limit cycles and, under certain operating conditions, may even be responsible for causing the combustor to become unstable under nominally stable conditions.

Nomenclature

C = autocorrelation function, defined in Eq. (1)
d = correlation dimension, defined in Eq. (4)
f = instability frequency
L = distance between fuel injector and the flame
m = number of data points
$\dot{m}$ = mass flow rate
p = pressure
R = scaling factor, see Eqs. (3) and (4)
r = Euclidean distance, see Eq. (2)
T = period of oscillations, $1/f$
u = velocity
τ = time delay
ϕ = equivalence ratio

Subscripts

$'$ = fluctuating quantity
$\bar{}$ = mean quantity

Introduction

THE occurrence of detrimental instabilities in lean, premixed combustors continues to hinder the development of modern gas turbines.[1–3] These instabilities arise from interactions between oscillatory flow and heat release processes in the combustor and often lead to large-amplitude, organized oscillations of the combustor's flowfields. These oscillations are undesirable because they significantly reduce the lifetime and regions of operability of the combustor.

To prevent the onset of these instabilities or, at least, minimize their detrimental effects (e.g., through active control), an understanding of the processes responsible for initiating and sustaining them is needed. That is, an understanding of the mechanism(s) that are responsible for initiating instabilities is needed in order to provide engineers with insight on how to avoid them in the design stage. An understanding of the nonlinear processes that control the steady-state or transient limit-cycle oscillations of the unstable system is needed in order to develop capabilities for predicting the amplitude of an instability or in the development and optimization of active control methodologies, respectively.

As a result of extensive experimental and theoretical work, the mechanisms responsible for initiating instabilities, and the conditions under which these instabilities occur, appear to be reasonably well understood. Specifically, it has been shown that these instabilities are likely initiated by a mechanism involving interactions between heat release, pressure, and reactive mixture composition oscillations.[3–5]

The current understanding of the nonlinear processes that control the limit-cycle oscillations in these combustors is much less complete, however. For example, there currently do not exist any capabilities for predicting the dependence of the instability amplitude upon operating conditions or geometric parameters. Furthermore, there is little understanding of other nonlinear phenomenon that have been reported, such as hysteresis in stability boundaries[3] or unstable mode selection.[5]

This paper describes the results of an experimental investigation of limit-cycle oscillations in a lean, premixed combustor that was performed to address these issues. Specifically, it presents data that describe the features of combustor pressure oscillations under stable and unstable operating conditions, the manner in which the combustor transitions from stability to instability, and the important factors controlling the instability amplitude. The paper is organized in the following manner: The following section briefly describes the experimental facility and then presents combustor pressure data that were measured under stable and unstable conditions. Next, it discusses the strong dependence of the amplitude of the limit-cycle oscillations upon the combustor inlet velocity. Finally, it characterizes the manner in which the combustor transitions from stability to instability with changes in operating conditions.

Characterization of Limit-Cycle Oscillations

The data presented in this paper were measured in a lean, premixed gas turbine combustor simulator (see Fig. 1), which is described in detail in Refs. 5 and 6. The facility consists of inlet, mixing, combustor, and exhaust sections. During a test, high-pressure air enters the variable length inlet section and mixes with gaseous fuel in the mixing section to form a reactive mixture that is supplied to the combustor. The mixture reacts at the bluff-body stabilized flame in the combustor section, and the hot combustion products exit the combustor through the exhaust section. The natural longitudinal

Received 2 February 2000; revision received 28 May 2001; accepted for publication 3 July 2001.

*Assistant Professor, School of Aerospace Engineering, 270 Ferst Drive; tim.lieuwen@aerospace.gatech.edu. Member AIAA.

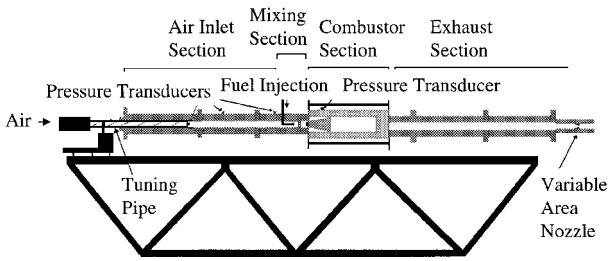

Fig. 1 Schematic of the investigated lean, premixed combustor simulator.

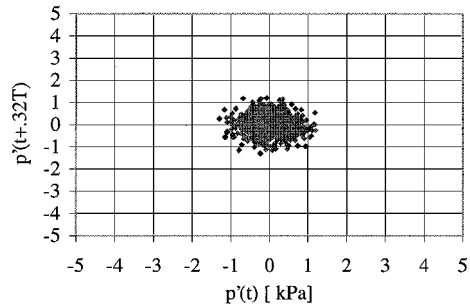

Fig. 2 Typical state-space evolution of the combustor pressure during stable operation ($\bar{u}$ = 24 m/s, $\bar{m}$ = 11.8 g/s, $\bar{\phi}$ = 0.89).

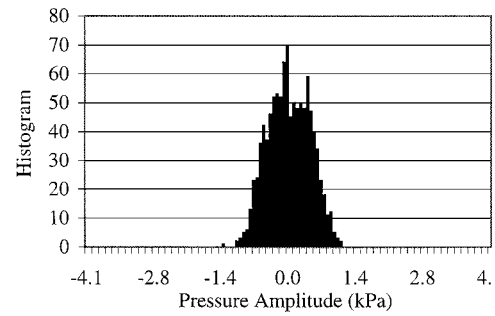

Fig. 3 Probability density function of combustor pressure for the operating conditions of Fig. 2.

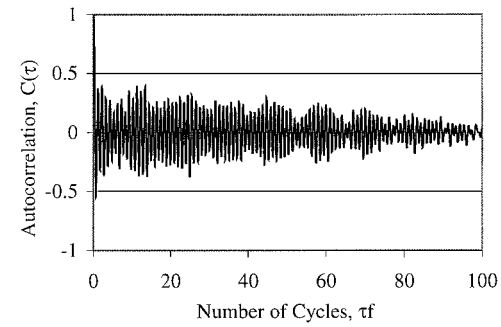

Fig. 4 Dependence of the autocorrelation of combustor pressure upon the number of cycles of oscillation at the operating conditions of Fig. 2 (the number of cycles plotted on the abscissa is based on a period of 630 Hz).

acoustic frequencies of the system are approximately multiples of 100 Hz (i.e., 100, 200, 300, ... Hz), and excitation of the first seven of these modes has been observed under different test conditions.[5] These oscillations were measured by four Model 211B5 Kistler pressure transducers mounted along the inlet section and combustor. The specific data presented next were obtained from the combustor mounted pressure transducer that was sampled at 2000 Hz.

The rest of this section presents data that characterize the basic temporal and statistical features of these combustor pressure oscillations during stable and unstable operation. We consider first the state-space evolution of the pressure under stable operating conditions. The state-space representation of the data is useful because it allows one to readily examine and compare the oscillations over a large number of cycles (in contrast, in examining the time evolution of the data it is difficult to examine more than a few cycles at a time or to compare successive cycles). The state space of an N degree-of-freedom (DOF) system is characterized at each instant by the vector $[x(t)\ \ \mathrm{d}x(t)/\mathrm{d}t \cdots \mathrm{d}^{N-1}x(t)/\mathrm{d}t^{N-1}]$, e.g., a two-DOF harmonic oscillator is characterized at each instant in time by the vector $[x(t)\ \ \mathrm{d}x(t)/\mathrm{d}t]$. Such a characterization of discretely sampled experimental data where only a single variable [e.g., $x(t)$] is measured requires numerical differentiation of the data, however, and is, thus, very sensitive to noise and measurement errors. Consequently, experimental time series are typically characterized with time-delay embedding methods.[7,8] The basic idea of this method is to construct the vector $[x(t)\ \ x(t+\tau)\ \ x(t+2\tau)\ \ \cdots\ \ x(t+n\tau)]$ from the measured data $x(t)$, where $n-1$ is the "embedding" dimension and τ is an arbitrary time delay.[7] The value of n that is needed to characterize the time series depends upon the number of DOFs of the system. For the majority of our results, a two-dimensional vector was found to adequately characterize the pressure time series (i.e., an examination of the plots of three-dimensional phase portraits revealed no significantly new features of the phase orbit).

Figure 2 plots the typical evolution of the unsteady combustor pressure $p'(t)$ during stable operation and shows that the majority of data points cluster around the fixed point $[p'(t)\ \ p'(t+0.32T)] = [0\ \ 0]$ (the choice of $\tau = 0.32T$ is somewhat arbitrary; similar results are obtained for other values). The scatter of the data about this fixed point reflects the fact that, even under stable conditions, the pressure is executing low-amplitude oscillations. The statistical characteristics of these oscillations are illustrated by the probability density function (PDF) of $p'(t)$ in Fig. 3. Figure 3 shows that the pressure distribution peaks at $p'(t) \approx 0$ and has a nearly Gaussian distribution about this mean. As will be shown next, this PDF is qualitatively different from the bimodal type PDFs observed under unstable operating conditions.

Further insight into the nature of the pressure oscillations can be obtained by examining their autocorrelation $C(\tau)$, which is defined next and illustrated in Fig. 4.

$$C(\tau) = \frac{\int p'(t)p'(t+\tau)\,\mathrm{d}t}{\int p'^2(t)\,\mathrm{d}t} \tag{1}$$

Several items should be noted from Fig. 4. First, note the oscillatory characteristics of $C(\tau)$. They reflect the oscillations of the system's natural acoustic modes, which are excited by background noise. Next, note the rapid drop in the envelope of $C(\tau)$ from its initial value of $C(\tau) = 1$ to a maximum value of $C(\tau) \approx 0.4$. This rapid drop reflects the presence of noise in the time series that has a small correlation time relative to the period of oscillations. These two observations suggest that the measured $p'(t)$ is composed of a superposition of noise and oscillations of the pressure at one or more of the natural acoustic frequencies of the system. Finally, note the monotonically decreasing envelope of $C(\tau)$ with increasing number of cycles. This drop in $C(\tau)$ is caused by damping in the system and reflects the system's finite "memory" because of the presence of dissipative processes in the system [note that the rate of decrease of $C(\tau)$ for a linear oscillator can be directly related to the amount of system damping[9]].

Consider next the characteristics of the pressure oscillations under unstable operating conditions. In this case the fixed point $[p'(t)\ \ p'(t+\tau)] = [0\ \ 0]$ is unstable, and the orbit is repelled from this point toward a new stable limit cycle. This loss of stability of the fixed point is reflected in the structure of the PDFs of the combustor pressure (see Fig. 5). The figure plots these PDFs at two different instability amplitudes. These PDFs resemble those of a signal consisting of a superposition of harmonic oscillations and noise. A comparison shows that the PDF with a single peak at $p' = 0$ in Fig. 3 has evolved into a bimodal PDF with peaks at nonzero pressure amplitudes in Fig. 5. The absolute value of the pressure at which these peaks occur roughly corresponds to the amplitude of the

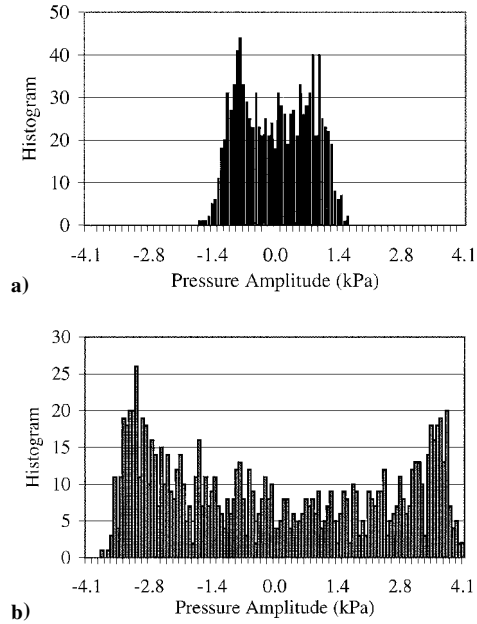

Fig. 5 Probability density functions of combustor pressure during unstable operation ($\bar{m}$ = 11.8 g/s, $\bar{\phi}$ = 0.89, f = 630 Hz, $\bar{u}$ = 26 and 31 m/s in Figs. 5a and 5b, respectively).

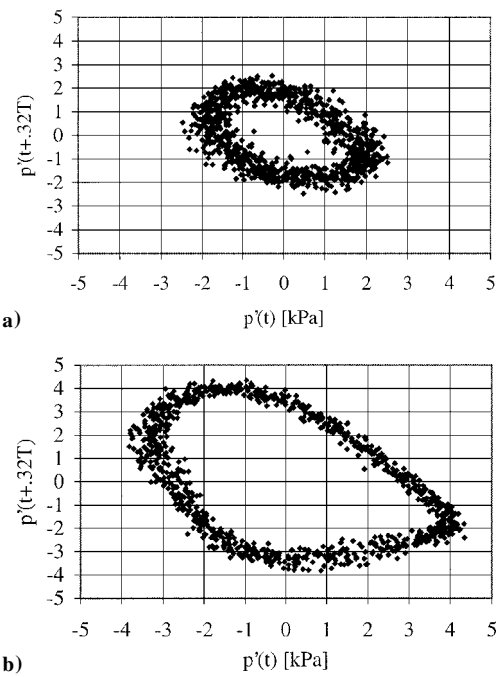

Fig. 6 State-space evolution of combustor pressure during unstable operation ($\bar{m}$ = 11.8 g/s, $\bar{\phi}$ = 0.89, f = 630 Hz , $\bar{u}$ = 31 and 33 m/s in Figs. 6a and 6b, respectively).

limit cycle. More insight into the characteristics of the limit-cycle oscillations can be obtained by examining their phase portraits at two different instability amplitudes (see Fig. 6). Purely sinusoidal oscillations exhibit elliptical phase orbits. Figure 6 shows that in the lower amplitude case the orbit is nearly elliptical, whereas in the larger-amplitude case the shape is somewhat distorted as a result of the generation of harmonics of the fundamental instability frequency by nonlinear processes.

Note also the scatter in the data in Fig. 6. This data scatter shows that the pressure oscillations do not exactly repeat themselves from one cycle to the next, i.e., they show that there is cycle-to-cycle variability in the limit-cycle oscillations. Such variability can arise from either 1) the nonlinear processes controlling the low-DOF oscillations (see also Refs. 8 and 10) that are the subject of this investigation or 2) background noise (e.g., turbulent fluctuations). Extensive analysis of the data has not given any indications that this cyclic variability reflects a deterministic, low-dimensional system dynamic. For example, extensive examination of the data has shown that the deviations are uncorrelated from one cycle to the next (see also data in Ref. 11; it should be noted, however, that another study[12] has reported that the variability is correlated from one cycle to another). These results suggest that the cyclic variations arise from background disturbances with correlation times that are short relative to the period of oscillations, i.e., processes that may be idealized as random forcing insofar as their effect on the self-excited oscillations that are of interest are concerned.

Further evidence that this cyclic variability does not reflect the presence of chaotic oscillations or a low-dimensional strange attractor is provided by examination of the "dimension" of the pressure oscillations. The value of this dimension essentially reflects the number of degrees of freedom of the system. For example, a system executing the periodic orbit $p'(t) = A\sin(\omega t)$ has a dimension d of one, and a system executing oscillations composed of two independent modes generally has a dimension of two. Turbulent fluctuations are often typified by a large number of degrees of freedom, and purely random processes have an infinite dimension. An orbit with a fractional dimensional (e.g., $d = 1.3$) typically displays complex behavior that may be indicative of chaotic oscillations.[7,13]

The underlying dimension of our pressure data was estimated using the Grassberger–Procaccia correlation dimension.[7] Because the algorithm for determining this dimension has been discussed extensively in the general dynamical systems literature[7] and in the specific context of combustion instabilities,[8,10] it will be only briefly discussed here. The basic steps in the determination of the correlation dimension of a time series record composed of m data points are as follows: 1) define an $n+1$ dimensional vector $\Pi(t)$ of the pressure at delayed times τ, e.g., $\Pi(t) = [p'(t)p'(t+\tau)p(t+2\tau)p(t+n\tau)]$; 2) determine the Euclidean distance r_{ij} between the vector defined by the ith and jth row of $\Pi(t)$, e.g., the distance r_{12} between the data points at $t = t_1$ and t_2 is

$$r_{12} = \sqrt{(p(t_1) - p(t_2))^2 + (p(t_1+\tau) - p(t_2+\tau))^2 + \cdots} \quad (2)$$

3) define a quantity R that ranges in value between the minimum and maximum values of r_{ij}; 4) for a given value of i, determine the number of values $N_i(R)$ of j for which $r_{ij} < R$; 5) define the correlation sum $C(R)$:

$$C(R) = \frac{1}{m}\sum_{i=1}^{m} N_i(R) \quad (3)$$

6) finally, define the pointwise correlation dimension $d(R)$:

$$d(R) = \frac{\log_{10} C(R)}{\log_{10} R} \quad (4)$$

For the procedure to converge, the value of the embedding dimension n must be sufficiently larger than the underlying dimension d. For our data a value of $n \geq 4$ was found to yield good results. Figure 7 plots the typical dependence of the pointwise

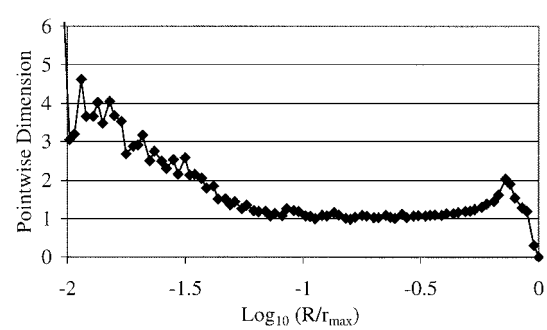

Fig. 7 Dependence of the pointwise Grassberger–Procaccia correlation dimension upon scale ($\bar{u}$ = 17 m/s, $\bar{m}$ = 11.8 g/s, $\bar{\phi}$ = 0.89).

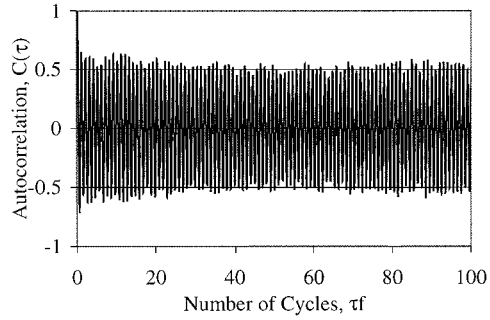

Fig. 8 Dependence of the autocorrelation of the combustor pressure upon the number of cycles for the operating conditions shown in Fig. 6a.

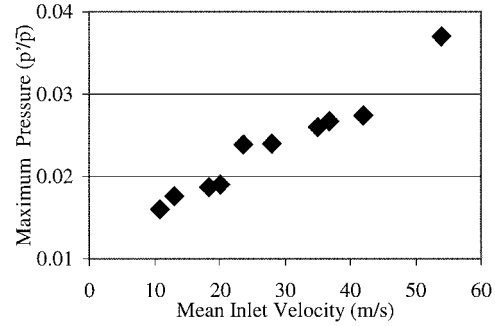

Fig. 9 Experimentally determined dependence of the maximum pressure amplitude upon the mean inlet velocity ($\bar{m}$ = 6.1–21.1 g/s, $\bar{\phi}$ = 0.65–1, f = 100–700 Hz, $\bar{p}$ = 1–10 atm, inlet length = 104–164 cm).

correlation dimension upon R. The figure shows that the correlation dimension has a constant, integer value of $d \approx 1$ in the range $-1.3 < \log_{10}(R/r_{\max}) < -0.3$, i.e., over one order of magnitude of $R/r_{\max}$. This and other similar results imply that the combustor pressure is executing a one-dimensional orbit.[7] This result provides additional evidence that the cyclic variability does not reflect the presence of a low-dimensional strange attractor. Noise in the data is the cause of the steady rise in the dimension d with decreasing radius R. The calculated dimension value is inaccurate below a value of $\log_{10} R/r_{\max} \sim -1.7$ because d approaches the value of the imbedding dimension ($n = 4$) that was used to obtain this result. A more accurate determination of d at smaller scales requires a considerably larger imbedding dimension n.

Before concluding this section, the features of the autocorrelation $C(\tau)$ of the pressure under unstable conditions are presented and compared with the autocorrelations of data obtained under stable conditions. A typical plot of $C(\tau)$ is presented in Fig. 8. Comparison of Figs. 4 and 8 reveals two common features shared by these autocorrelations: 1) the oscillatory characteristics of $C(\tau)$ and 2) the rapid drop in $C(\tau)$ from its initial value of one after one cycle (because of noise in the data with short correlation times). In view of the preceding discussion, it is likely that the noise in the pressure signal which is responsible for the rapid drop in $C(\tau)$ in Fig. 8 is also responsible for the cyclic variability shown in Fig. 6.

Comparing the dependence of the envelope of $C(\tau)$ upon the time delay τ reveals a qualitative difference between these curves, however. Specifically, the envelope of $C(\tau)$ monotonically decreases in Fig. 4 and remains relatively constant in Fig. 8. This constant amplitude envelope of $C(\tau)$ shows that the oscillations are highly correlated with one another during an instability at least over the first 100 cycles of oscillation.

There has been some discussion in the combustion instability literature on distinguishing between low-amplitude, self-excited oscillations and those oscillations exhibited by a linearly stable combustor driven by noise (e.g., Ref. 14). The discussion in the preceding paragraphs suggests that the qualitative differences between the pressure autocorrelations of the two systems can be used to distinguish between the two situations.

Dependence of the Instability Amplitude upon Combustor Parameters

Correlation of the Instability Amplitude

Having discussed several of the qualitative features of the pressure time series data, we next consider the important factors that determine the steady-state limit-cycle amplitude. Extensive data have been published that present the dependence of the instability amplitude upon operating conditions and geometric parameters in lean, premixed gas turbine combustors, e.g., see Refs. 1–3 and 6. However, no correlation of the amplitude has been determined that would describe its simultaneous dependence upon several relevant parameters, such as pressure, equivalence ratio, or fuel injector location. Although we have not found any such universal correlation either, we have found that the combustor inlet velocity plays a very significant role in determining the instability amplitude over the entire parameter space studied in our combustor (i.e., equivalence ratio = 0.65–1, combustor pressure = 1–10 atm, combustor inlet length = 104–164 cm, instability frequency = 100–700 Hz, and reactants mass flow rate = 6.1–21.1 g/s, see also Ref. 5); see Fig. 9. Figure 9 plots the dependence of the maximum pressure amplitude upon the inlet velocity, e.g., if pressure oscillations with amplitudes of 0.5, 1, and 1.5% of the mean were measured in the 10–12 m/s velocity range, then the 1.5% value is plotted in the figure. The figure shows that over the entire parameter space the maximum normalized pressure amplitude is a monotonically increasing function of the inlet velocity, i.e.,

$$p'/\bar{p}|_{\max} \propto \bar{u} \tag{5}$$

Thus, although the instability amplitude may take a whole range of values at any given inlet velocity, these data show that it takes on larger values at higher velocities.

This result suggests that the inlet velocity plays a significant role in determining the amplitude at which the instability saturates. Assuming that the acoustic pressure p' and velocity u' are approximately proportional, this result also suggests that $u'/\bar{u}$ is an important nondimensional parameter which controls the amplitude of the limit-cycle oscillations. These observations support the conclusions of several theoretical studies[5,15,16] that have suggested that $u'/\bar{u}$ type nonlinearities control the nonlinear dynamics of unstable gas turbine combustors.

By further pursuing this observation, some insight into the important physical processes that saturate the limit-cycle amplitude can be obtained by examining which of them exhibit a nonlinear dependence upon $u'/\bar{u}$. For example, it is known from other studies that $u'/\bar{u}$ is an important parameter that controls the nonlinear response of a flame front[15] and the reactive mixture composition[5,16] to flow perturbations. Thus, these data suggest that combustion process nonlinearities can play a role in saturating the instability amplitude. In the same way $u'/\bar{u}$ is an important parameter controlling the nonlinear damping of acoustic waves at a rapid flowfield expansion (see Ref. 17 and references therein), suggesting that nonlinear boundary conditions could also play an important role in the nonlinear dynamics of the combustor. Finally, it is known that it is the parameters $u'/\bar{c}$ or $p'/\bar{p}$, not $u'/\bar{u}$, which control the lowest-order nonlinear response of gas dynamical processes to flow perturbations.[18] Thus, this result suggests that gas dynamic nonlinearities do not play a significant role in the limit-cycle oscillations of our combustor.

Relationship Between the Instability Frequency and Amplitude

The data presented in the prior subsection showed that the inlet velocity plays an important role in the limit-cycle amplitude, i.e., that it has a strong influence upon the nonlinear characteristics of the system. Previous studies of the instability mechanism in this combustor have shown that the inlet velocity also plays an important role upon the conditions under which instabilities occur and their frequency (through its affect on the time required for the reactive mixture to convect from the fuel injection point to the flame), i.e., that it also has a strong influence upon the linear characteristics of the combustor. Specifically, it has been suggested on experimental[3,5] and

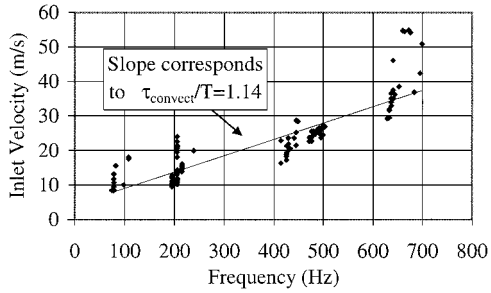

Fig. 10 Experimentally determined relationship between instability frequency and inlet velocity ($\dot{m}$ = 6.1–21.1 g/s, $\bar{\phi}$ = 0.65–1, $\bar{p}$ = 1–10 atm, inlet length = 104–164 cm).

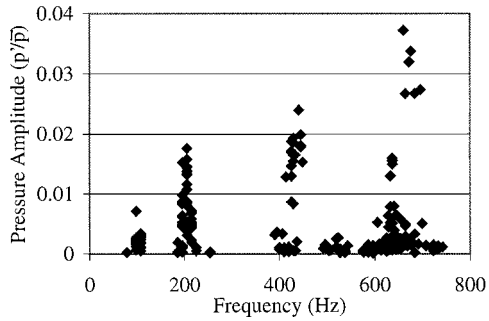

Fig. 11 Dependence of instability amplitude upon frequency of instability ($\dot{m}$ = 6.1–21.1 g/s, $\bar{\phi}$ = 0.6–1, $\bar{p}$ = 1–10 atm, inlet length = 104–164 cm, $\bar{u}$ = 10–60 m/s).

theoretical[4] grounds that the following expression approximately describes the conditions under which the combustor is unstable[5,6]:

$$\tau_{\text{convect}}/T = (L/\bar{u})f = C_n \tag{6}$$

where C_n is a function of combustor geometry. Assuming that L and C_n are constants, manipulation of Eq. (6) shows that the frequency of the destabilized combustor mode is proportional to the mean inlet velocity, i.e.,

$$f \propto \bar{u} \tag{7}$$

Thus, Eqs. (6) and (7) predict that higher frequency combustor modes will be excited at higher inlet velocities. This dependence can be seen in the data (see Fig. 10). Figure 10 clearly shows that, in general, low-frequency instabilities are excited at low inlet velocities and high-frequency instabilities are excited at higher inlet velocities. The slope of the least-squares line through the data can be predicted quite accurately from purely theoretical considerations.[5]

These data show that the inlet velocity has a significant effect on the linear (conditions under which instabilities occur and their frequency) and nonlinear (amplitude of oscillations) characteristics of the combustor. If we combine the result shown in Fig. 9 and Eq. (5) (i.e., $p'/\bar{p}|_{\max} \propto \bar{u}$) with the result shown in Fig. 10 and Eq. (7), (i.e., $f \propto \bar{u}$), we obtain the interesting and rather counterintuitive result that the maximum amplitude of the instability is proportional to its frequency, i.e.,

$$p'/\bar{p}|_{\max} \propto f \tag{8}$$

In other words, the preceding results and Eq. (8) suggest that larger-amplitude instabilities will occur at higher frequencies, a trend that is clearly exhibited in our data (see Fig. 11). Because acoustic damping processes increase with frequency of oscillation (e.g., both viscous damping and radiation losses increase as the square of the frequency), one might expect that, in general, the largest-amplitude instabilities will occur at the lowest frequencies. The preceding discussion and Eq. (8) provide a clear explanation for the counterintuitive trend shown in Fig. 11, however. Although clearly this trend could not continue to arbitrarily high frequencies, these data strongly suggest that the inlet velocity affects both the linear and nonlinear characteristics of the instability.

Characterization of Bifurcations

This section discusses the qualitative features of the experimentally observed bifurcations in the combustor's stability characteristics. Recall that a bifurcation refers to a qualitative change in the dynamics of the system with a change in a system parameter. In this section we are referring to the bifurcation where the fixed point at $[p'(t)\,p'(t+\tau)] = [0\ \ 0]$ shown in Fig. 2 becomes unstable and "repels" the pressure orbit toward a new, stable limit cycle, such as is shown in Fig. 6. Such bifurcations can be classified as either sub- or supercritical[7] (see Fig. 12). This figure plots the dependence of the oscillatory amplitude upon a system parameter that controls the system's stability (this could be, for example, the inlet velocity, combustor pressure, etc.). As shown in these examples, when the system undergoes a sub- or supercritical bifurcation, the steady-state amplitude of the oscillations changes abruptly and continuously, respectively, with changes in parameter values. Hysteresis occurs in systems with subcritical bifurcations. This hysteresis can be seen in Fig. 12b by noting that the parameter value where the amplitude of the oscillations discontinuously changes depends upon whether the system parameter is increasing or decreasing. Finally, systems with subcritical bifurcations that are operating under linearly stable conditions can become unstable if they are excited with large-amplitude disturbances. For example, reference to Fig. 12b shows that the system is linearly stable when the system parameter lies between −0.5 and 0 but, if disturbed with sufficient amplitude, will jump up to the stable, oscillatory branch. This behavior is often referred to as "triggering" in the combustion instability literature.[18]

Both of these bifurcations have been observed in our combustor under different operating conditions. Figures 13 and 14 illustrate typical examples of observed super- and subcritical bifurcations. Although both types of bifurcations have been observed and discussed in several prior experimental and theoretical studies, we present these data because they show that both types of bifurcations can occur in the same combustor at different operating conditions. It was generally observed that supercritical bifurcations occurred under higher inlet velocity, lower mean combustor pressure (e.g., 1–5 atm) operating conditions where the excited instability frequencies were in the 400–700 Hz range. Conversely, subcritical bifurcations were more often observed under low inlet velocity, high-pressure conditions where the excited instabilities were in the 100–200 Hz

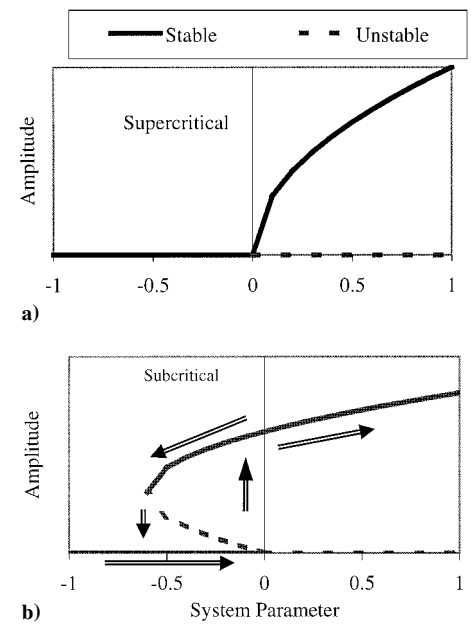

Fig. 12 Dependence of oscillatory amplitude upon a system parameter that affects its stability characteristics (e.g., mean inlet velocity) for sub- and supercritical bifurcations.

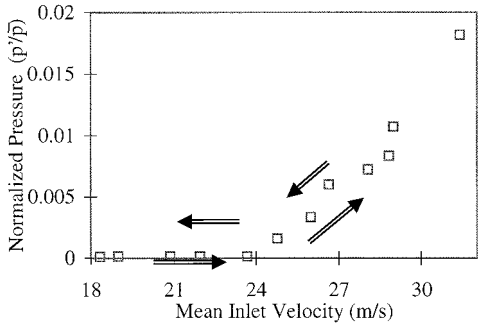

Fig. 13 Dependence of combustor pressure upon the mean inlet velocity ($\bar{m}$ = 11.8 g/s, $\bar{\phi}$ = 0.89, f = 630 Hz).

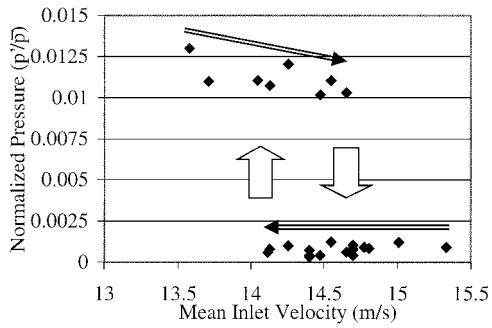

Fig. 14 Dependence of the fluctuating pressure amplitude upon the mean inlet velocity ($\bar{m}$ = 16 g/s, $\bar{\phi}$ = 0.85, f = 204 Hz).

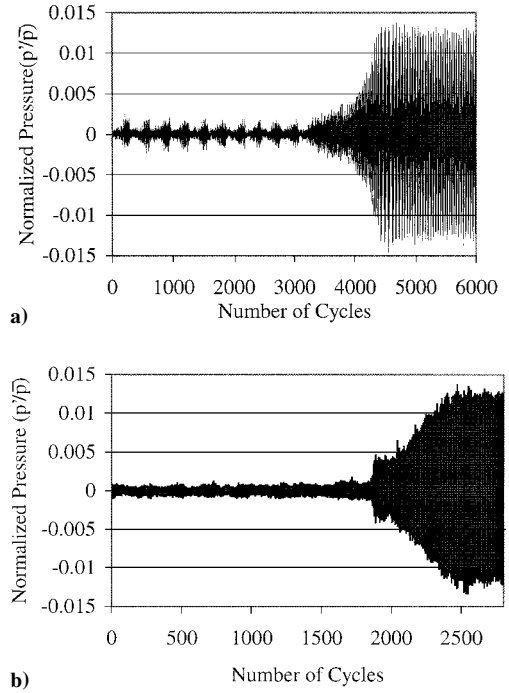

Fig. 15 Dependence of combustor pressure amplitude upon number of cycles ($\bar{m}$ = 16 g/s, $\bar{\phi}$ = 0.85, f = 204 Hz, $\bar{u}$ = 14.1 and 14.4 m/s in Figs. 15a and 15b, respectively).

range. The fundamentally different nature of the bifurcations shown in Figs. 13 and 14 suggests that the important system nonlinearities in unstable combustors can also fundamentally change with operating conditions. This result shows that nonlinear models that describe the combustor dynamics under certain operating conditions may not work at others.

The arrows drawn in Figs. 13 and 14 indicate how the pressure amplitude changes with inlet velocity. Note the hysteresis in the stability boundary in Fig. 14, i.e., the velocity at which the system changes its stability characteristics depends upon whether it is increasing or decreasing. Also, the vertical arrows indicating the bifurcation point are drawn in the figure with a broad width to indicate that the exact bifurcation point varied from test to test. We postulate that this variability in bifurcation point is caused by the effects of background disturbances that cause the combustor's instantaneous state to fluctuate between stable and unstable when the system is operating very near the "mean" stability boundary. Indeed, the following behavior was often observed when the combustor was operated near the stability boundary of a subcritical bifurcation point: if the velocity was changed to a value close to the stability boundary, the pressure would initially continue to oscillate in a low-amplitude, somewhat random fashion for a certain amount of time. However, at some instant later the pressure amplitude would suddenly increase before reaching a steady state with large-amplitude, coherent oscillations. Two examples of this behavior are illustrated in Fig. 15. It should be emphasized that the operating conditions were not changed over the time period during which data were taken during this test. Rather, the sudden jump in pressure amplitude shown in the figures occurred spontaneously. This result suggests that background combustor noise can destabilize the system under "nominally" stable conditions. Depending upon the exact operating point, the length of time that typically elapsed before the jump in amplitude occurred could range from a few seconds to several minutes.

Comparing the transient characteristics of the oscillations in Figs. 15a and 15b shows that they are completely different. For example, the oscillations smoothly and monotonically increase in Fig. 15a, whereas they first jump up rapidly, then stay relatively constant, and then smoothly increase in Fig. 15b. Observations of these transitions in several other tests revealed that this transient period could differ markedly from test to test at the same operating conditions, suggesting that it has some intrinsically stochastic characteristics. Note also the "beating" of the pressure oscillations in Fig. 15a before the amplitude suddenly increases. As shown in Fig. 15b, however, the sudden jump in pressure amplitude was not always preceded by this beating phenomenon.

As just discussed, linearly stable systems with subcritical bifurcations can exhibit triggering, i.e., they can become unstable if disturbed with sufficient amplitude. This triggering phenomenon was also observed in some of our tests under similar conditions as those in Figs. 14 and 15. Such triggering was manifested by the combustor transitioning from stable to unstable after a sudden change in operating conditions or temporary reignition of the pilot fuel-oxygen flame.

Conclusions

This paper has presented time series data of combustor pressure oscillations that were measured in a gas turbine combustor simulator. It has been shown that these limit-cycle oscillations vary from cycle to cycle, but also have a component that exhibits significant temporal coherence. Based upon dynamical systems and statistical analysis, it was suggested that the cyclic variability was caused by forcing of the system by background noise. It has also shown that the inlet section velocity not only plays a role in the linear stability characteristics of the combustor (as shown in prior studies[3–6]), but also affects the amplitude of the limit-cycle oscillations. Finally, it has presented the nature in which the combustor transitions from stable to unstable operation and shown that the characteristics of this bifurcation can affect the amount of hysteresis in the system's stability boundaries and its sensitivity to background disturbances under stable operating conditions.

In closing, this paper has only presented an analysis of steady-state time series data. It seems likely that further insight into the characteristics of the system could be obtained by examining its transient dynamics, e.g., analyzing the time series data in Fig. 15a between 3200–4400 cycles.

Acknowledgments

This work was partially supported by A6TSR under contract # 99-01-5R075.

References

[1]Cohen, J., and Anderson, T., "Experimental Investigation of Near-Blowout Instabilities in a Lean, Premixed Combustor," AIAA Paper 96-0819, Jan. 1996.

[2]Broda, J. C., Seo, S., Santoro, R. J., Shirhattikar, G., and Yang, V., "An Experimental Investigation of Combustion Dynamics of a Lean, Premixed Swirl Injector," *Proceedings of the Twenty-Seventh International Symposium on Combustion*, Combustion Inst., Pittsburgh, PA, 1998, pp. 1849–1856.

[3]Straub, D. L., and Richards, G. A., "Effect of Fuel Nozzle Configuration on Premix Combustion Dynamics," American Society of Mechanical Engineers, Paper 98-GT-492, June 1998.

[4]Lieuwen, T., and Zinn, B. T., "The Role of Equivalence Ratio Oscillations in Driving Combustion Instabilities in Low NOx Gas Turbines," *Proceedings of the Twenty-Seventh International Symposium on Combustion*, Combustion Inst., Pittsburgh, PA, 1998, pp. 1809–1816.

[5]Lieuwen, T., "Investigation of Combustion Instability Mechanisms in Premixed Gas Turbines," Ph.D. Dissertation, Georgia Inst. of Technology, Atlanta, Aug. 1999, pp. 85–111.

[6]Torres, H., Lieuwen, T., Johnson, C., Daniel, B. R., and Zinn, B. T., "Experimental Investigation of Combustion Instabilities in a Gas Turbine Combustor Simulator," AIAA Paper 99-0712, Jan. 1999.

[7]Hilborn, R. C., *Chaos and Nonlinear Dynamics*, Oxford Univ. Press, New York, 1994, pp. 407–417.

[8]Sterling, J. D., "Nonlinear Analysis and Modeling of Combustion Instabilities in a Laboratory Combustor," *Combustion Science and Technology*, Vol. 89, Nos. 1–4, 1993, pp. 167–179.

[9]Lin, Y. K., and Cai, G. Q., *Probabilistic Structural Dynamics: Advanced Theory and Applications*, McGraw–Hill, New York, 1995, pp. 1–35.

[10]Keanini, R., Yu, K., and Daily, J., "Evidence of a Strange Attractor in Ramjet Combustion," AIAA Paper 89-0624, Jan. 1989.

[11]Lieuwen, T., "Phase Drift Characteristics of Self Excited, Combustion Driven Oscillations," *Journal of Sound and Vibration*, Vol. 242, No. 5, 2001, pp. 893–905.

[12]Jacobsen, C., "System Identification for Models of Lean Premix Combustion Instability," *Proceedings of the Workshop on Dynamics and Control of Combustion Instabilities in Propulsion and Power Systems*, California Inst. of Technology, Pasadena, Nov. 1997.

[13]Culick, F. E. C., Paparizos, L., Sterling, J., and Burnley, V., "Combustion Noise and Combustion Instabilities in Propulsion Systems," *Proceedings of AGARD Conference on Combat Aircraft Noise*, AGARD CP 512, 1992.

[14]Hibshman, J. R., Cohen, J. M., Banaszuk, A., Anderson, T. J., and Alholm, H. A., "Active Control of Combustion Instability in a Liquid-Fueled Sector Combustor," American Society of Mechanical Engineers, Paper 99-GT-215, June 1999.

[15]Dowling, A. P., "Nonlinear Self Excited Oscillations of a Ducted Flame," *Journal of Fluid Mechanics*, Vol. 346, 1997, pp. 271–290.

[16]Peracchio, A. A., and Proscia, W. M., "Nonlinear Heat Release/Acoustic Model for Thermo-Acoustic Instability in Lean Premixed Combustors," American Society of Mechanical Engineers, Paper 98-GT-269, June 1998.

[17]Dowling, A. P., and Hughes, I. J., "Sound Absorption by a Screen with a Regular Array of Slits," *Journal of Sound and Vibration*, Vol. 156, No. 3, 1992, pp. 387–405.

[18]Culick, F. E. C., Burnley, V., and Swenson, G., "Pulsed Instabilities in Solid-Propellant Rockets," *Journal of Propulsion and Power*, Vol. 11, No. 4, 1995, pp. 657–665.